Measurements of aerosol phase function and vertical backscattering coefficient using a charge-coupled device side-scatter lidar

Zongming Tao,[1,2] Dong Liu,[2,*] Zhenzhu Wang,[2] Xiaomin Ma,[1] Qingze Zhang,[1] Chenbo Xie,[2] Guangyu Bo,[2] Shunxing Hu,[2] and Yingjian Wang[2]

[1]*New Star Institute of Applied Technology, Hefei, Anhui, 230031, China,*
[2]*Key Laboratory of Atmospheric Composition and Optical Radiation, Anhui Institute of Optics and Fine Mechanics, Chinese Academy of Sciences, Hefei, Anhui, 230031 China*
[*]*dliu@aiofm.ac.cn*

Abstract: By using a charge-coupled device (CCD) as the detector, side-scatter lidar has great potential applications in the near range atmospheric detection. A new inversion method is proposed for CCD side-scatter lidar (Clidar) to retrieve aerosol phase function and vertical backscattering coefficient. Case studies show the retrieved results from Clidar are in good agreements with those obtained from other instruments. It indicates that the new proposed inversion method is reliable and feasible and that the Clidar is practicable.

©2013 Optical Society of America

OCIS codes: (010.1110) Aerosols; (280.3640) Lidar; (290.5820) Scattering measurements.

References and links

1. R. J. Charlson, S. E. Schwartz, J. M. Hales, R. D. Cess, J. A. Coakley, Jr., J. E. Hansen, and D. J. Hofmann, "Climate forcing by anthropogenic aerosols," Science **255**(5043), 423–430 (1992).
2. A. Ansmann, D. Althausen, U. Wandinger, K. Franke, D. Miiller, F. Wagner, and J. Heintzenberg, "Vertical profiling of the Indian aerosol plume with six-wavelength lidar during INDOEX: a first case study," Geophys. Res. Lett. **27**(7), 963–966 (2000).
3. D. M. Winker, J. Pelon, and M. P. McCormick, "The CALIPSO mission: Spaceborne lidar for observation of aerosols and clouds," Proc. SPIE **4893**, 1–11 (2003).
4. F. Mao, W. Gong, and J. Li, "Geometrical form factor calculation using Monte Carlo integration for lidar," Opt. Laser Technol. **44**(4), 907–912 (2012).
5. J. E. Barnes, S. Bronner, R. Beck, and N. C. Parikh, "Boundary layer scattering measurements with a charge-coupled device camera lidar," Appl. Opt. **42**(15), 2647–2652 (2003).
6. J. E. Barnes, N. C. Sharma, and T. B. Kaplan, "Atmospheric aerosol profiling with a bistatic imaging lidar system," Appl. Opt. **46**(15), 2922–2929 (2007).
7. F. G. Fernald, "Analysis of atmospheric lidar observations: some comments," Appl. Opt. **23**(5), 652–653 (1984).
8. Z. Tao, D. Liu, C. Xie, X. Ma, X. Meng, S. Hu, and Y. Wang, "A numerical inversion method for CCD side-scatter lidar," in *Proceedings of International Conference on Remote Sensing, Environment and Transportation Engineering* (Academic, 2013), pp. 250–252.
9. T. Nakajima, G. Tonna, R. Rao, P. Boi, Y. Kaufman, and B. Holben, "Use of sky brightness measurements from ground for remote sensing of particulate polydispersions," Appl. Opt. **35**(15), 2672–2686 (1996).

1. Introduction

Aerosol plays a strong role in global climate change both directly, by affecting Earth's radiation balance, and indirectly, by affecting cloud properties [1]. Understanding their contribution to climate change requires the vertical distribution of the aerosol [2]. As aerosol types, chemistry, concentrations are highly variable and strongly altitude-dependent, measurements of aerosol properties as a function of altitude are especially important. The majority of aerosol exists in a layer of few kilometers near the Earth's surface which has a very important impact to human beings. This aerosol-rich layer is generally called the atmospheric (or planetary) boundary layer. Remote sensing techniques using a variety of instruments have been applied to aerosol detection. Sun photometers provide the total column aerosol content, indicative of the aerosol properties integrated through the entire atmosphere.

#200916 - $15.00 USD Received 6 Nov 2013; revised 10 Dec 2013; accepted 13 Dec 2013; published 10 Jan 2014
(C) 2014 OSA

Backscatter lidar is capable of providing range-resolved atmospheric profiles continuously, making them valuable tool in the remote sensing of atmospheric aerosol [3]. But the backscatter lidar system has a shortcoming in the lower hundreds of meters because of the overlap factor caused by the configuration of the transmitter divergence and receiver's field-of-view(FOV) at ranges close to the instrument [4]. This limits the backscatter lidar to be applied to the near-range measurement, especially for the fixed vertical-pointing apparatus.

Appling a CCD camera detector, a side-scatter lidar, in which the camera is spatially separated to look the laser beam at a certain distance, is a different configuration compared with the backscatter lidar. The Clidar solves the overlap problem caused by backscatter lidar, and is especially suitable to measure aerosol in the near range [5,6]. This paper is focused on how to obtain the aerosol phase function and how to solve the side-scatter lidar equation.

In the following paragraph, a numerical inversion and experimental method for Clidar is proposed. The skyradiometer retrieved aerosol phase function is used to make comparison. Combining the backscattering lidar measurement simultaneously, the vertical aerosol backscattering coefficient obtained by Clidar is also retrieved and validated.

2. Apparatus

The diagram of Clidar is shown in Fig. 1. For the side-scatter Clidar configuration, the lidar equation can be described as [5]

$$P(\theta) = \frac{P_0 K A}{D} \beta(\theta) T_z T_r d\theta \tag{1}$$

where $P(\theta)$ is the received power at height z and scattering angle θ by a pixel, K is a system constant including the optical and electronic efficiency and A is the aperture of the receiving optics, T_z and T_r are the total (aerosol and molecular) atmospheric transmittance from the laser to distance z and from distance z along the slant path R to the CCD receiver, respectively. $\beta(\theta)$ is the total atmospheric side-scattering coefficient. Because of $\theta = \pi/2 + \gamma$, $d\theta$ (equal to $d\gamma$) is FOV of one pixel. The specifications of the Clidar system are summarized in Table 1.

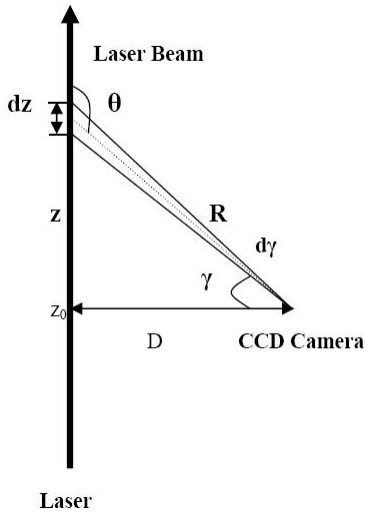

Fig. 1. The measurement configuration of the Clidar.

#200916 - $15.00 USD Received 6 Nov 2013; revised 10 Dec 2013; accepted 13 Dec 2013; published 10 Jan 2014
(C) 2014 OSA

Table 1. The key specifications of the Clidar system

Laser	(Quantel Brilliant) Nd:YAG
Wavelength	532 nm
Pulse energy	200 mJ
Repetition rate	10 Hz
Divergence	0.5 mrad
Detector	(SBIG) ST-8300M
Pixel array	3352 × 2532
Pixel size (μm)	5.4 × 5.4
Angle per pixel (deg/pix)	~0.02
Dark (electrons/s/pixel)	< 0.5e at 0 °C
Full well capacity (electrons)	25,500
A/D convecter (bits)	16
Cooling	Single TE, Active Fan, ~35 °C Delt
Temperature regulation (°C)	Closed loop, ± 0.1
Wide-angle lens	Walmexpro f/2.8
Lens focal length (mm)	14
CCD sensor	Kodak KAF-8300
Quantum efficiency (532nm)	~55%
Interference Filter	(Semrock corporation)
Bandwidth (nm)	25.6
Peak transmittance	~95%
Computer	(Lenovo × 200)

For the CCD receiver, side-scatter lidar signals record by different pixels. From the geometry, the spatial resolution dz is expressed as

$$dz = \frac{R^2}{D} d\theta \tag{2}$$

For the Clidar system, the FOV of each pixel $d\theta$ is measured by calibration experiments; the measured $d\theta$ is an approximate constant, so the spatial resolution dz increases with the slant distance R .

By comparing the Eqs. (1) and (2) with corresponding backscatter lidar equations, Clidar has two main difference aspects with the backscatter lidar. One is that the spatial resolution is not constant, the other is received power is not $1/R^2$ dependence. The cancellation of the $1/R^2$ dependence has a beneficial consequence for the dynamic range of the Clidar system. For the short range detection, such as the atmospheric boundary layer, Clidar can provide a fine vertical resolution due to the elaborate optics design.

3. Methodology

As to the backscatter lidar equation, Fernald provided an interactive inversion solution for two-component atmosphere [7]. But to the Clidar equation, Fernald's inversion method is not suitable, due to the difference of the atmospheric transmittance and the adoption of the aerosol phase function. The side-scattering coefficient $\beta(\theta)$ and the total scattering coefficient β_s have the relationship as

$$\beta(\theta) = pf(\theta)\beta_s \tag{3}$$

where $pf(\theta)$ is the aerosol phase function. If the backscattering coefficient is known, the side-scattering coefficient $\beta(\theta)$ can be expressed as

$$\beta(\theta) = \frac{\beta(\pi)}{pf(\pi)} pf(\theta) = f(\theta)\beta(\pi) \tag{4}$$

$f(\theta) = pf(\theta)/pf(\pi)$ is the relative aerosol phase function. The Clidar equation in forward-scattering ($\theta \le 90^0$), can be written as

#200916 - $15.00 USD Received 6 Nov 2013; revised 10 Dec 2013; accepted 13 Dec 2013; published 10 Jan 2014
(C) 2014 OSA

$$P(\theta)=\frac{P_0KA}{D}[\beta_1(\pi)f_1(\theta)+\beta_2(\pi)f_2(\theta)]\exp\{-[\int_0^z(\alpha_1(z')+\alpha_2(z'))dz' +\int_z^{z_0}(\alpha_1(z')+\alpha_2(z'))dz'/\cos\theta]\}d\theta \quad (5a)$$

for backward-scattering ($90^0 \ge \theta \ge 180^0$), the equation can be written as

$$P(\theta)=\frac{P_0KA}{D}[\beta_1(\pi)f_1(\theta)+\beta_2(\pi)f_2(\theta)]\exp\{-[\int_0^z(\alpha_1(z')+\alpha_2(z'))dz' +\int_{z_0}^{z}(\alpha_1(z')+\alpha_2(z'))dz'/\cos(\pi-\theta)]\}d\theta \quad (5b)$$

where $\alpha(z)$ is the extinction coefficient, subscripts "1" and "2" stand for aerosol and molecule, respectively. The first transmission terms without scattering angle θ in both Eqs. (5a) and (5b) indicate the path from the laser to the scatter region. The other parts of the transmission terms indicate the path from the scatter region to the CCD camera.

In general, for Eqs. (5a) and (5b), there are three unknown variables, i.e. phase function, backscatter and extinction coefficient of aerosol. This is the similar scenario one met as the retrieval of the backscatter lidar [7]. A prior assumption has to be given, i.e. lidar ratio (extinction-to-backscatter ratio) of the aerosol, in order to reduce the unknowns. The value of 50 Sr is used as lidar ratio at 532 nm wavelength in our algorithm. Thus, if the phase function is determined, the backscatter and extinction coefficient of the aerosol can be retrieved by Clidar.

3.1 Phase function retrieval

Using horizontal pointing configuration of Clidar and backscatter lidar, a retrieval method of the aerosol phase function is proposed as the following. Let Clidar and backscatter lidar point horizontally at the same time. In this case, the constant aerosol extinction coefficient can be assumed due to the homogeneity.

Let θ_c as a reference point, the molecular backscatter coefficient, extinction coefficient and phase function can be determined from a standard atmosphere. Aerosol backscatter coefficient and extinction coefficient can obtained from backscatter lidar in the simultaneous experiment.

At the reference point θ_c , Eqs. (5a) and (5b) become

$$P(\theta_c)=\frac{P_0KA}{D}[\beta_1(\pi)f_1(\theta_c)+\beta_2(\pi)f_2(\theta_c)]\exp\{-[(\alpha_1+\alpha_2)z_c+(\alpha_1+\alpha_2)(z_0-z_c)/\cos\theta_c]\}d\theta_c \quad (6a)$$

$$P(\theta_c)=\frac{P_0KA}{D}[\beta_1(\pi)f_1(\theta_c)+\beta_2(\pi)f_2(\theta_c)]\exp\{-[(\alpha_1+\alpha_2)z_c+(\alpha_1+\alpha_2)(z_c-z_0)/\cos(\pi-\theta_c)]\}d\theta_c \quad (6b)$$

z_c is the distance corresponding to θ_c . C can be determined by

$$C=\frac{P(\theta_c)}{[\beta_1(\pi)f_1(\theta_c)+\beta_2(\pi)f_2(\theta_c)]d\theta_c} \quad (7)$$

The attenuated side-scatter, $\beta'(\theta)$, can then be computed

$$\beta'(\theta)=\frac{P(\theta)}{C} \quad (8)$$

#200916 - $15.00 USD Received 6 Nov 2013; revised 10 Dec 2013; accepted 13 Dec 2013; published 10 Jan 2014
(C) 2014 OSA

From Eqs. (6a) and (6b), Eq. (8) can be written as

$$\beta'(\theta) = [\beta_1(\pi) f_1(\theta) + \beta_2(\pi) f_2(\theta)] \exp\{-[(\alpha_1 + \alpha_2)(z - z_c) + (\alpha_1 + \alpha_2)((z_0 - z)/\cos\theta - (z_0 - z_c)/\cos\theta_c)]\} d\theta \quad (9a)$$

$$\beta'(\theta) = [\beta_1(\pi) f_1(\theta) + \beta_2(\pi) f_2(\theta)] \exp\{-[(\alpha_1 + \alpha_2)(z - z_c) + (\alpha_1 + \alpha_2)((z - z_0)/\cos(\pi - \theta) - (z_c - z_0)/\cos(\pi - \theta_c))]\} d\theta \quad (9b)$$

Firstly, $\theta_c \approx 180^0$ is selected as the reference point, i.e. $f_1(\theta_c) = 1$. Using the numerical inversion method [8], the relative phase function of aerosol within the scatter angles from 90° to 180° can retrieved from Eq. (9b). Then, setting $\theta_c = 90^0$ as the reference point, using above method, the relative phase function of aerosol within the scatter angles from 0° to 90° can retrieved from Eq. (9a). There is a proportional constant between the relative phase function and the phase function of aerosol, this proportional constant could be computed by normalization or by scaled to match the known phase function of aerosol from other instruments. In our algorithm, this constant is computed by scaled to match the known phase function of aerosol from POM02 measurement at 500 nm wavelength.

3.2 Vertical backscatter coefficient retrieval

Aerosol phase function is determined by size distribution, refractive index and component, is not dependent on the concentration. Assuming the aerosol phase function as uniform in the planetary boundary layer, the backscatter coefficients cloud be retrieved from Clidar as shown in the following way. Let Clidar point vertically, and keep the polarization angle the same for both the vertical and horizontal measurements. In this case, the aerosol phase function measured by Clidar in horizontal pointing is used to retrieve the vertical aerosol backscatter coefficient.

Selecting θ_c as a reference point, the aerosol backscatter coefficient value at this point can be obtained from the data of backscatter lidar in the simultaneous experiment. The molecular backscatter, extinction coefficients and phase function can be determined from a standard atmosphere. Using above numerical inversion method, the backscatter and extinction coefficient of aerosol can be retrieved from Eqs. (5a) and (5b) if the lidar ratio is given.

4. Case study and validation

In the evening on Sep.9, 2013, the aerosol phase function was measured with Clidar pointed horizontally. The distance between the CCD and the laser beam was 7.91 m. The sky condition of this evening was overcast, the aerosol extinction coefficient was 0.88 km^{-1} near the surface, the corresponding visibility was around 4.5 km. Because of the total view angle of the CCD camera is about 64° (64° in horizontal, 52° in vertical), the center axis of the CCD camera was put on three directions in turn in order to get 0° to 180° scattering signals. First, CCD center axis was pointed to 150° scattering angle, with the exposure time of 100s. Second, CCD center axis was pointed to 90° scattering angle, with the same exposure time. Last, CCD center axis was pointed to 30° scattering angle, with the exposure time of about 10s. Figure 2(a) shows the signals measured at three directions. The black solid line in Fig. 2(b) is the retrieved aerosol phase function using the new proposed method discussed above. In order to validate the results, the aerosol phase function measured before the sunset by skyradimeter (POM02) at the same location is plotted in red solid line in Fig. 2(b). The skyradimeter is an important instrument of SKYNET project, and the SKYRAD.pack version 4.2 software [9] was used to retrieve aerosol optical and microphysical properties including aerosol phase function at the wavelengths of 340nm, 380nm, 400nm, 500nm, 675nm, 870nm, and 1020nm by using a radiative transfer code and an inversion scheme.

#200916 - $15.00 USD Received 6 Nov 2013; revised 10 Dec 2013; accepted 13 Dec 2013; published 10 Jan 2014
(C) 2014 OSA

Skyradiometer uses the Sun radiation, while Clidar uses laser. Skyradiometer measures the columnar atmospheric aerosol properties, while the Clidar measures phase function of aerosol which lies in the laser beam path. Figure 2(b) shows that the retrieved aerosol phase function from Clidar has a good agreement with the POM02 measurement. Within 0° to 15° scattering angle, aerosol phase function changes greatly with scattering angle. It is difficult to detect aerosol phase function precisely. So for above and following two cases, the retrievals from 0° to 15° in the scattering angle are omitted.

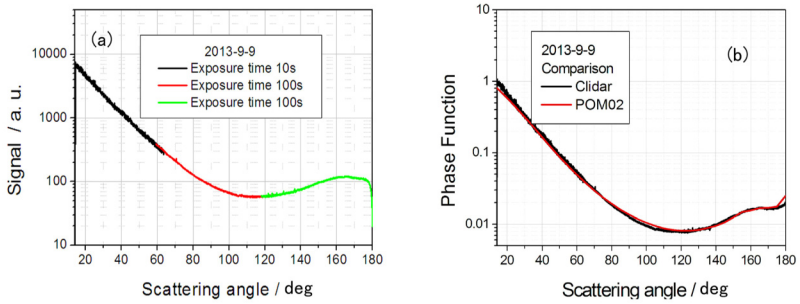

Fig. 2. Measurement by Clidar on Sep. 9, (a) raw signal (b) retrieved aerosol phase function

In the evening on Sep. 16, 2013, the aerosol phase function was measured again for further comparison. The distance between the CCD and the laser beam was 6.71 m. The sky condition of this evening was clear, the aerosol extinction coefficient was 0.33 km^{-1} near the surface, the corresponding visibility was around 11.5 km. The CCD center axis was put on three directions in turn. The detailed exposure time and CCD pointers are the same as the last experiment on Sep.9, 2013. Figure 3(a) shows the signals measured at three directions. Comparison with POM02 in Fig. 3(b) again indicates a good agreement except the data point at about 15° and 150° scattering angles.

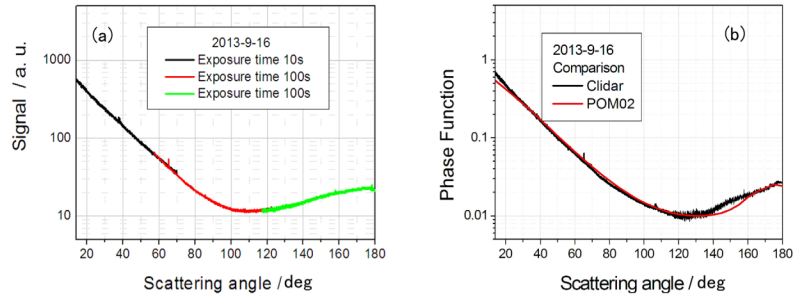

Fig. 3. Measurement by Clidar on Sep. 16, (a) raw signal (b) retrieved aerosol phase function

In the evening on Oct.15, 2013, the Clidar was pointed vertically to measure the aerosol backscatter coefficient profile. The distance between CCD and laser beam was 20.89 m, and the sky condition of this evening was clear. The CCD center axis was put on 65° tilting angle, with the exposure time of about 100s. Meanwhile, two backscatter lidars worked horizontally and vertically respectively at the same place and POM02 was also deployed at the same location to provide the aerosol phase function. Figure 4 is the signal measured by the Clidar at 19:40 at local standard time (LST), Fig. 4(a) is the image of the vertical transmitting laser beam, Fig. 4(b) is the signal profile with pixel number and Fig. 4(c) is the signal profile with altitude. Figure 5(a) and 5(b) show the retrieved aerosol backscattering coefficients by different instruments at 19:40 and 20:40 LST, respectively. The black solid lines in Figs. 5(a) and 5(b) are the retrieved aerosol backscatter coefficient profiles using vertical-pointing backscatter lidar, the red solid lines in Figs. 5(a) and 5(b) are the aerosol backscattering coefficient profiles from the Clidar using the above proposed method, and the black stars are

#200916 - $15.00 USD Received 6 Nov 2013; revised 10 Dec 2013; accepted 13 Dec 2013; published 10 Jan 2014
(C) 2014 OSA

the aerosol backscattering coefficient near the surface by the horizontal-pointing backscatter lidar.

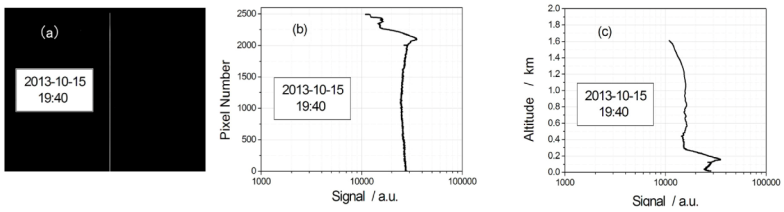

Fig. 4. Signal measured by Clidar on Oct. 15th, (a) the image of laser beam, (b) the signal profile versus pixel number and (c) the signal profile versus altitude

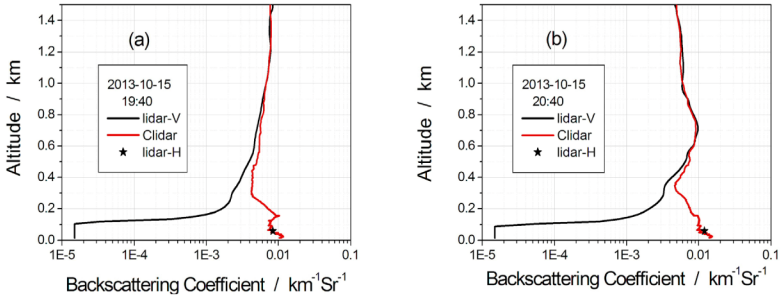

Fig. 5. Retrieved profile of aerosol backscattering coefficient by vertical-pointing backscatter lidar, Clidar and backscatter lidar pointing horizontally. (a) measured at 19:40 LST, (b) measured at 20:40 LST

For both Clidar and backscatter lidar retrieval methods, the aerosol extinction-to-backscatter ratio is assumed 50 Sr, the molecular extinction coefficient and backscattering coefficient are from the U. S. standard atmosphere model(1976). From Fig. 5(a), one can see that between 0.9 km and 1.5 km altitude, the aerosol backscattering coefficients measured by the Clidar and vertical-pointing backscatter lidar are in a good agreement. From the surface to about 0.9 km, the aerosol backscattering coefficient retrieved from vertical-pointing backscatter lidar is not correct due to the overlap factor, so there is a big difference between vertical-pointing backscatter lidar and Clidar results. The Clidar results have a good agreement with the horizontal-pointing backscatter lidar retrieval at 50m above ground level (AGL). In practice, for avoiding the obstructions, the laser beam has an elevation angle of 2 degrees when making the horizontal measurement. The slant range corresponding to 50 m in vertical is about 1.5 km horizontally. Figure 5(b) shows the similar results as Fig. 5(a). The aerosol backscattering coefficient in the near surface changed from 0.0084 $km^{-1}Sr^{-1}$ to 0.012 $km^{-1}Sr^{-1}$ during this one hour duration.

By combining vertical-pointing backscatter lidar and Clidar measurement, retrieved backscattering coefficient profile from surface to 7 km AGL at 19:40 LST and 20:40 LST on Oct.15, 2013 are plotted in Fig. 6. From Fig. 6, one can see that there were two aerosol layers separated at about 2 km in this evening. Within one hour, aerosol backscattering coefficient in the above aerosol layer changed little, while the backscattering coefficient in the lower layer changed greatly in the vertical shape. In the very close surface, there is still variation of the aerosol in the vertical structure which can't be detected by the ordinary backscattering lidar due to the dead zone of the overlap factor, while the Clidar can reveal it.

#200916 - $15.00 USD Received 6 Nov 2013; revised 10 Dec 2013; accepted 13 Dec 2013; published 10 Jan 2014
(C) 2014 OSA

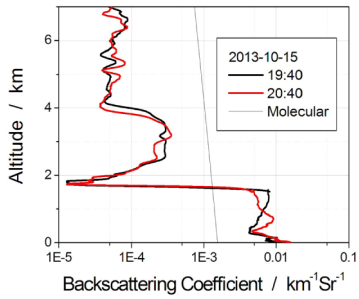

Fig. 6. Aerosol backscattering coefficient profiles retrieved by combined lidars

5. Discussion and conclusions

A new method of Clidar is proposed to detect the aerosol phase function. The aerosol phase function retrieved by a skyradiometer is used to make the comparison. In the comparison experiments, Clidar worked at nighttime in order to reduce background noise, while the aerosol phase function retrieved from the skyradiometer is before the sunset. This means that the comparison experiments is not simultaneous, but at the same place. From above two cases, aerosol phase function from Clidar and skyradiometer are consistence within 15° to 180° in scattering angle which indicates the composition and size distribution of aerosol not changing greatly within that time.

The errors in the aerosol phase function retrieval from Clidar are due to the background noise, interfering light, CCD dark current level, the model molecular parameters and so on. Based on the Clidar Eq. (9), the impact of the molecular phase function is getting smaller while aerosol backscattering coefficient is getting bigger. Aerosol backscattering coefficient in Fig. 3(b) is smaller than that in Fig. 2(b), so the deviation in Fig. 3(b) may be from molecular phase function variation.

The comparisons with POM02 in Figs. 2(b) and 3(b) show that the method in which aerosol phase function is retrieved by Clidar is feasible, and the retrieved aerosol phase function is reliable. Figure 3(b) shows that aerosol backscattering coefficient profile retrieved by Clidar is feasible and reliable too. The Clidar is a good supplement to the backscatter lidars. Combined these two techniques, the vertical profile of aerosol backscattering coefficient can be measured from the very beginning of the surface and the overlap factor of the backscatter lidar can also be obtained for the fixed vertical-pointing lidars.

Acknowledgments

This work was supported by the National Natural Science Foundation of China under Grant No. 41175021, No. 41075016 and No.41005014. The skyradiometer POM02 retrieval is provided by the SKYNET Hefei observatory.

#200916 - $15.00 USD Received 6 Nov 2013; revised 10 Dec 2013; accepted 13 Dec 2013; published 10 Jan 2014
(C) 2014 OSA